Theor. Appl. Climatol. 65, 181–196 (2000)

Theoretical and Applied Climatology

LIM – Institut für Meteorologie, Universität Leipzig, Leipzig, Germany

On the Influence of Surface Heterogeneity on the Bowen-Ratio: A Theoretical Case Study

K. Friedrich[+], **N. Mölders,** and **G. Tetzlaff**

With 8 Figures

Received April 21, 1999
Revised December 10, 1999

Summary

The influence of surface heterogeneity on spatial distribution, temporal development, and on the domain-average of the ratio between sensible and latent heat-flux (Bowen-ratio) is investigated for synthetic landscapes of differing degrees of surface heterogeneity. In so doing, simulations are performed applying a 3-dimensional non-hydrostatic mesoscale model. The synthetic landscapes consist of patches of sandy loam covered by *mixed forest* and loamy soil covered by *grass*. The results of the numerical experiments substantiate that land-surface distributions will non-linearly influence the Bowen-ratio if patches of equal type exceed a certain size. Moreover, the heterogeneity of the upwind region may play a role. Similarity coefficients show that the surface type dominating a landscape does not necessarily determine the mean Bowen-ratio representative for this area. Thus, when applying the strategy of dominant surface type, the margin of error in the regional Bowen-ratio depends on the horizontal resolution of the model or on available data.

1. Introduction

The ratio between sensible and latent heat-fluxes (Bowen-ratio) is a regional characteristic that depends on the underlying surface and meteorological conditions. On the one hand, the Bowen-ratio serves as a climatological quantity that characterizes an area. In this case, the Bowen-ratio is given as a long-term mean value valid for a region of given geo-ecological characteristics (e.g., dominant land-use and soil-type, latitude, elevation, continental location, drainage basin, etc.) for a given length of time (e.g., month, vegetation period, year, decade, etc.). On the other hand, the Bowen-ratio can be regarded as an actual property characterizing the *atmosphere-surface-interaction*. In this sense, the Bowen-ratio may be used, for instance, to simplify measurements of the surface energy-budget (e.g., Müller et al., 1993; Foken et al., 1997).

Using the Bowen-ratio as a climatologically characteristic quantity of a region implies that the Bowen-ratio depends on micrometeorological conditions. In this climatological sense, it does not depend on the individual upwind meteorological history of air flow and upwind terrain type. In this case, the Bowen-ratio would always be the same for the same set of local conditions such as climate, insolation, geographical latitude, elevation, land-use-type, and soil-type. However, there are clues that, especially on shorter time scales, the latter does not hold true. Several investigators have found that the local energy-budget is not closed exactly, even over the long term. This so-called 'non-closure' of the local energy-budget is assumed to be a result of surface heterogeneity on the upwind-side (e.g., Panin et al., 1998).

In the determination of a regional Bowen-ratio, whereby Bowen-ratio maps are devised as

[+] Present affiliation: DLR, Institut für Physik der Atmosphäre, Oberpfaffenhofen, Postfach 1116, 82230 Wessling, Germany.

well as in a numerical modeling situation, a resolution has to be chosen in which the Bowen-ratios are to be determined. To ascertain the Bowen-ratios on a given resolution, a strategy of dominant surface type is usually applied as a simplifying method. This means that for an area of several square kilometers, the dominant surface type is assumed to be representative for determining the water- and energy-fluxes at the earth's surface, and thus, the Bowen-ratio. Natural surfaces, however, are heterogeneous on virtually all scales. Hence, it is to be expected that, under similar geographical and climatic conditions, regional Bowen-ratios vary with the variation of these surfaces. Several authors (for a review, see Giorgi and Avissar, 1997) have shown that the strategy of dominant surface type may be inadequate in representing the surface forcing because of the great variety in soil-types and vegetation.

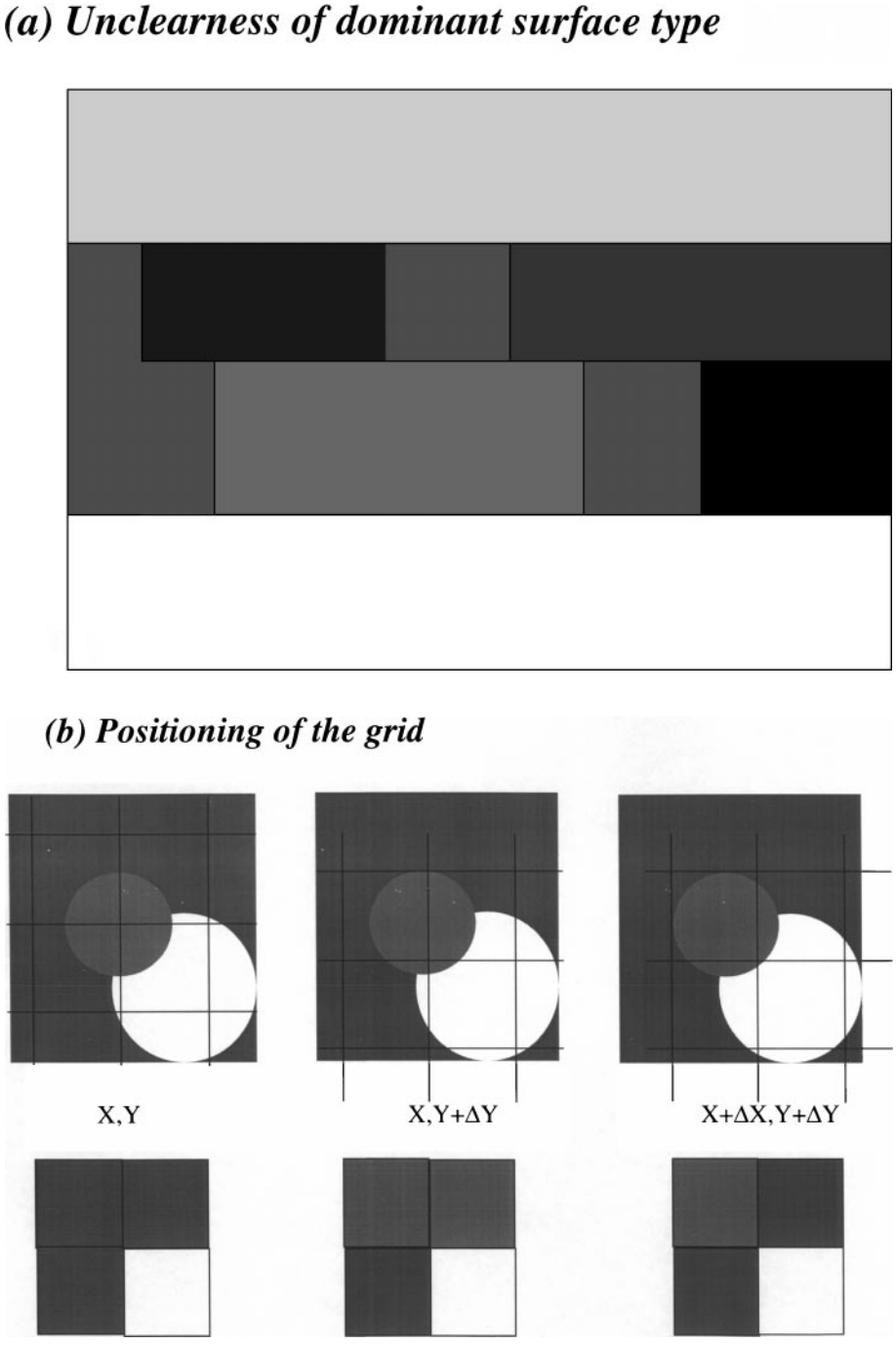

Fig. 1. Schematic illustrations of difficulties arising when applying the strategy of dominant surface type

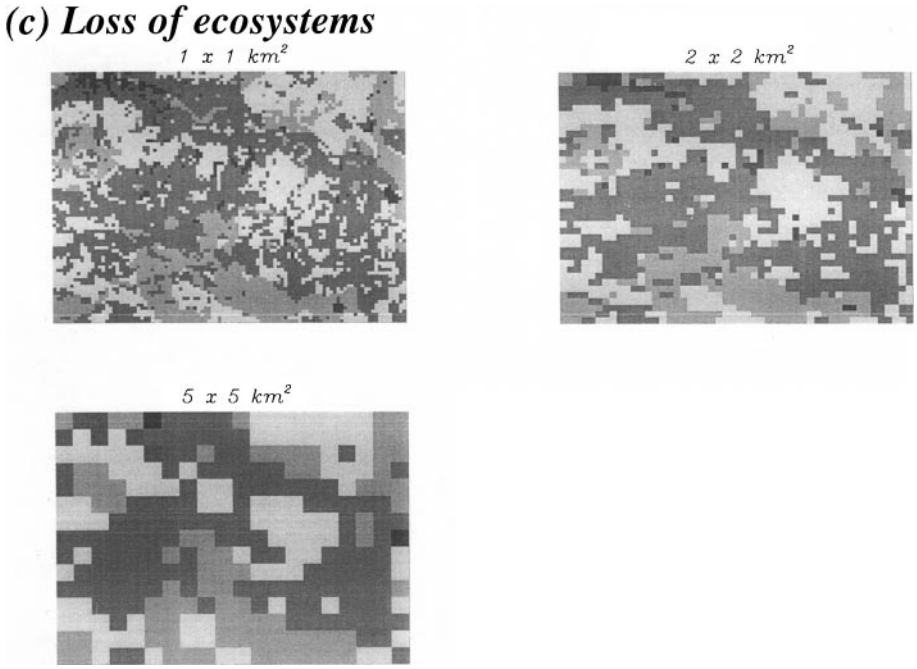

Fig. 1 (*continued*)

Apparently, in the case of a coarse resolution (of data or the model), applying the strategy of dominant surface type is dubious for many reasons. Two or more land-surface types cover areas of equal size (represented by the white and light grey stripe in Fig. 1a) and each of these areas exceed the coverage of all other surface types within the area under examination. Thus, the dominant surface type cannot be definitely determined and one of these ''dominant'' surface types has to be arbitrarily chosen to be representative for the area. Other difficulties arise from the respective choice of the grid-location or grid-resolution (Fig. 1b, c). As shown in Fig. 1b, a town (here represented by the medium-grey circle) similar in size to the grid-cells may be of subgrid-scale (Fig. 1b, left) or it may be the dominant land-use-type within this grid-cell depending on the positioning of the grid (Fig. 1b, right). If, in fact, the grid divides the town into two or more parts, the town may end up being of subgrid-scale in these grid-cells, if the strategy of dominant surface type is used (Fig. 1b, left). On the contrary, the town can be over-represented if, within the grid-cells, there are other land-use-types that extend less than the town (Fig. 1b, middle). Another major difficulty in the strategy of dominant surface type is illustrated in Fig. 1c. The number of different surface types (here represented by different colors) decreases with increasing grid-cell sizes or areas (Fig. 1c). Surface types of small horizontal extension (e.g., small eco-systems, a village, creeks, etc.) become subgrid-scale for coarser grid-resolutions and are ignored (Fig. 1c). Specifically, this means that in the regional Bowen-ratio for arid or semi-arid regions, for instance, the high evapotranspiration rate of oases, or, in mid-latitudes, the low evapotranspiration rate of dry and warm areas (e.g., open-pit mines, cities, etc.) can be suppressed by a coarse resolution (e.g., Mölders and Raabe, 1996). Thus, applying a croase grid resolution may lead to a loss of eco-systems or a falsely determined regional Bowen-ratio.

It is obvious that, to obtain a better representation of the Bowen-ratio, a finer grid resolution should be employed. Unfortunately, in numerical modeling this possibility is restricted not only by model parameterization limitations and the scarcity of meteorological, land-use and soil-type data to initialize the model, but also by computer performance (Mölders and Raabe, 1996). Determining a regional Bowen-ratio on the basis of geo-ecological parameters and micrometeorological climatic conditions depends on the available resolution of these quantities. Herein, the geo-ecological parameters, however,

are again often based on the strategy of dominant surface type.

According to the results of previous considerations and aforementioned studies, it is thus to be expected that a regional Bowen-ratio may be sensitive to both surface heterogeneity and probably to advective effects as well. Therefore, in our study the sensitivity of the regional Bowen-ratio to surface heterogeneity will be examined. Special focus will be given to whether or not there exists an impact of upstream-conditions on Bowen-ratio. If the Bowen-ratio is found to be independent of the upstream surface conditions, soil- and land-use-type data, elevation, soil moisture, near-surface windspeed, temperature, and humidity alone can be used to create regional maps of Bowen-ratios. Otherwise, such maps have to be calculated by 3-D-atmospheric models. To examine the influence of surface heterogeneity on a regional Bowen-ratio, numerical simulations are performed using the non-hydrostatic meteorological model GESIMA (**GE**esthacht's **SI**mulation **M**odel of the **A**tmosphere; Kapitza and Eppel, 1992; Eppel et al., 1995). In the various simulations, differing arrangements of *grass* and *forest* are assumed.

2. Model Description and Initialization

GESIMA and its modules are validated for a great range of situations (e.g., Claussen, 1988; Kapitza and Eppel, 1992; Eppel et al., 1995; Devantier and Raabe, 1996; Hinneburg and Tetzlaff, 1996; Mölders, 1998). The soil-vegetation module, for instance, was evaluated for different soil-types and meteorological conditions and its results were compared with those of other soil-vegetation models (e.g., Claussen, 1988; Mölders, 1998; Fritsch, 1999; Mölders and Kramm, 1999). GESIMA demonstrated that it is able to simulate the typical behavior associated with various land-use-types (Mölders, 1998).

The treatment of soil/vegetation/atmosphere interaction follows Deardorff (1978; see also Claussen, 1988; Eppel et al., 1995; Mölders, 1998). Homogeneous soil- and land-surface characteristics are assumed within a subgrid-cell. A force-restore method determines soil-wetness factors. At the surface, the fluxes of sensible and latent heat are calculated by applying a bulk-formulation. Transpiration of plants is considered by a Jarvis-type approach (1976). The soil heat-fluxes and soil temperatures are determined by a diffusion equation (Claussen, 1988; Eppel et al., 1995) where soil temperature at a depth of 1 m is held constant at the climatological value. The surface stress and near-surface fluxes of heat and water vapor are expressed in terms of dimensionless drag- and transfer-coefficients, applying the parametric model of Kramm et al. (1995). Above the atmospheric surface layer, the turbulent fluxes of momentum are calculated by a one-and-a-half-order closure scheme (Eppel et al., 1995). In all simulations, subgrid-scale surface heterogeneity is considered by an explicit subgrid-scheme (Seth et al., 1994; Mölders et al., 1996). This scheme uses a finer grid resolution than that used in the atmospheric model. On the subgrid, the water- and energy-fluxes, soil-wetness factors, as well as soil- and surface-temperature are calculated taking into account the subgrid soil-physical and plant-physiological characteristics. Coupling to the atmospheric grid-cell is performed by arithmetically averaging the subgrid-fluxes. Radiation transfer is calculated by a simplified two-stream method (Eppel et al., 1995).

The inner model domain (= test domain) encompasses $100\times100\,\mathrm{km}^2$. Hence, the test domain is of a size similar to grid-cells in mesoscale-α models or the resolution often applied in maps of Bowen-ratios covering, for instance, continental-sized areas. The horizontal resolution of the grid is $5\times5\,\mathrm{km}^2$, and that of the subgrid is $1\times1\,\mathrm{km}^2$ to allow for differing degrees of surface heterogeneity to be represented. The vertical resolution varies from 20 m close to the ground to 1 km at the top of the model which is at 12 km height. Eight levels are located below the 2 km height and 9 above. All simulations are integrated for a 24 hours period, where the first six hours serve as the adjusting phase.

To investigate the influence of surface heterogeneity on the regional Bowen-ratio, the initial conditions chosen are as simple as possible, namely, a homogeneously flat terrain on sea level which is assumed for all simulations. Moreover, all simulations are initialized by the same synthetic atmospheric profiles of air temperature and humidity. Here, a dry-adiabatic temperature profile is assumed, starting with an air temperature of 22 °C near the ground. To ensure cloud-

Table 1. *Surface Characteristics for Forest with a Sandy Loam Soil and a Grass Coverage with a Loam Soil after Eppel et al., 1995*

	Forest	*Grass*
Thermal conductivity $[10^{-6}\,m^2\,s^{-1}]$	0.7	0.73
Heat capacity $[10^6\,J\,K^{-1}\,m^{-3}]$	2.5	2.1
Albedo	0.15	0.25
Roughness length [m]	0.75	0.02
Field capacity weighted by upermost soil layer [m]	0.01	0.004
Capillarity $[kg\,m^{-3}\,s^{-1}]$	0.008	0.002
Maximum evaporation conductivity $[m\,s^{-1}]$	0.023	0.040
Emissivity	0.95	0.95

free conditions, relative humidity is chosen as 50% near the ground and decreases linearly to 1% at a height of 12 km. Surface pressure amounts to 1035.2 hPa. A geographical latitude of 51.5° N and June 21st are arbitrarily chosen for radiation calculation. Above the atmospheric boundary layer (ABL), a geostrophic westerly wind of 8 m/s is assumed. In addition, the soils are assumed to be fully water-saturated to avoid water limitation for evapotranspiration. At a 1 m depth, soil temperature is arbitrarily set equal to 6.9 °C. Table 1 lists the plant- and soil-specific parameters applied in this theoretical study.

3. Design of the Numerical Experiments

In our case study, the influence of surface heterogeneity on the regional Bowen-ratio is investigated assuming five different synthetic landscapes (Fig. 2). The first landscape, denoted as HOMF, consists of homogeneous *forest* on sandy loam. The second landscape, hereafter called HOMG, is homogeneously covered by *grass* grown on loam. In the following, *grass* is always assumed to go along with loam, and *forest* is assumed to stand on sandy loam, i.e., a different land-use distribution always goes along

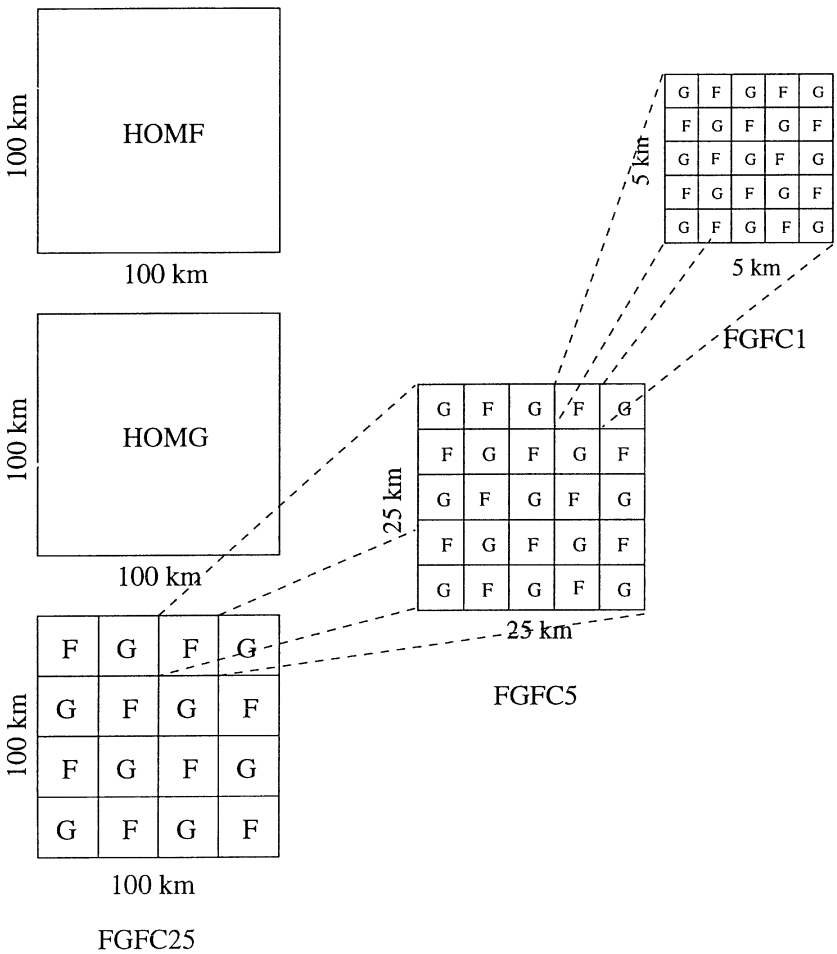

Fig. 2. Schematic view of surface distribution applied in this study. Here, HOMG and HOMF stand for the simulations with homogeneous *grass*, and *forest*, with the letters G and F representing *grass* and *forest*, respectively

with an altered soil distribution. Three further landscapes are designed with different checkerboard arrangements of *forest*- and *grass*-patches (Fig. 2). These landscapes are addressed as FGFC25, FGFC5, and FGFC1, respectively. Herein, the letters FGF represent the alternating *forest*- and *grass*-patches, and C stands for the checkerboard arrangement. The numbers give the length of the smallest *forest*-patch, e.g., the number 25 stands for a $25 \times 25\,\mathrm{km}^2$ *forest*-patch size (Fig. 2). Note that these synthetic landscapes FGFCx ($x = 1, 5, 25$) are designed that way purposely so that the respective landscape of greater heterogeneity does not replicate the landscape of the next highest degree of heterogeneity when applying the strategy of dominant surface types. The landscape FGFC25 represents an example for which an arbitrary decision has to be made on the representative surface type when applying the strategy of dominant surface types.

Simulations alternatively assuming these five different landscapes are performed. Hereafter, these simulations, as well as their results, will be addressed according to the name of the respective synthetic landscape. As mentioned above, all simulations are carried out under the same meteorological conditions with the same model configuration. Due to this modeling strategy the results will differ only in so far as differences exist in the underlying surface (e.g., heterogeneity) and their resulting effects on micrometeorological conditions.

The temperature and moisture states in the system *earth-atmosphere* evolve by fluxes which themselves depend on those states. The resultant non-linear dynamical system has modes of variability and statistical signatures that depend on the interactions of the energy- and water-budget (Entekhabi and Brubaker, 1995). The impact of surface heterogeneity on the Bowen-ratio will be examined by means of the temporal development of the domain-averaged water- and energy-fluxes, and by means of similarity coefficients.

4. Temporal Development

The temporal development is investigated by use of hourly domain-averages,

$$\overline{\chi}(t) = \frac{\sum_{i=1}^{n} \sum_{j=1}^{n} \chi_{i,j}(t)}{n^2}, \qquad (1)$$

where $\chi_{i,j}(t)$ stands for the values of the fluxes or other quantities of interest (e.g., latent and sensible heat-flux, net-radiation, soil heat-flux, Bowen-ratio, etc.) at each grid-point i, j at time t, and n^2 ($= 400$) is the number of grid-points within the inner model domain.

4.1 The Energy Budget

The *big-leaf/big-stomata*-approach, applied in GESIMA, assumes that, in the case of vegetation, (1) the soil is totally covered by plants, and (2) the exchange at the interface *earth-atmosphere* is accomplished at the top of the canopy (i.e., 7.5 m and 0.2 m for *forest* and *grass*, respectively). As given in Table 1, the roughness length of *forest* ($z_0 = 0.75$ m) exceeds that of *grass* ($z_0 = 0.02$ m). Additionally, the air temperatures established above the *forest*-patches differ from those above the *grass*-patches. Therefore, momentum-, and hence, heat- and moisture-fluxes differ at the interface *earth-atmosphere*.

In assessing the temporal development of the domain-averaged components of near-surface latent and sensible heat-fluxes, net-radiation, and soil heat-fluxes (Fig. 3a–d) it is indicated that the different surface distributions affect mainly the latent heat-flux in the morning and afternoon (Fig. 3a), while the greatest differences in domain-averaged net-radiation and sensible heat-flux occur between 10 LT and 14 LT (Fig. 3b, c). At 12 LT, the domain-averaged net-radiation and sensible heat-flux of HOMG and HOMF, for instance, differ by about $90\,\mathrm{W/m^2}$ and $100\,\mathrm{W/m^2}$, respectively (Fig. 3b, c). The domain-averaged soil heat-fluxes provided by HOMG, FGFC25, FGFC5, FGFC1 differ hardly at all, i.e., the domain-averaged soil heat-fluxes are insensitive to heterogeneity (Fig. 3d). HOMF and HOMG differ about $10\,\mathrm{W/m^2}$, i.e., the domain-averaged soil heat-fluxes are insensitive to surface-type (Fig. 3d). Note that all fluxes descending towards the surface are defined by a negative sign, while all fluxes going upward have a positive sign.

Since the domain-averaged net-radiation is governed by the albedo, α, of the prevailing land-use, the domain homogeneously covered by *forest* ($\alpha = 0.15$) yields the greatest net-radiation, while the domain homogeneously covered by *grass* ($\alpha = 0.25$) attains the lowest net-radiation

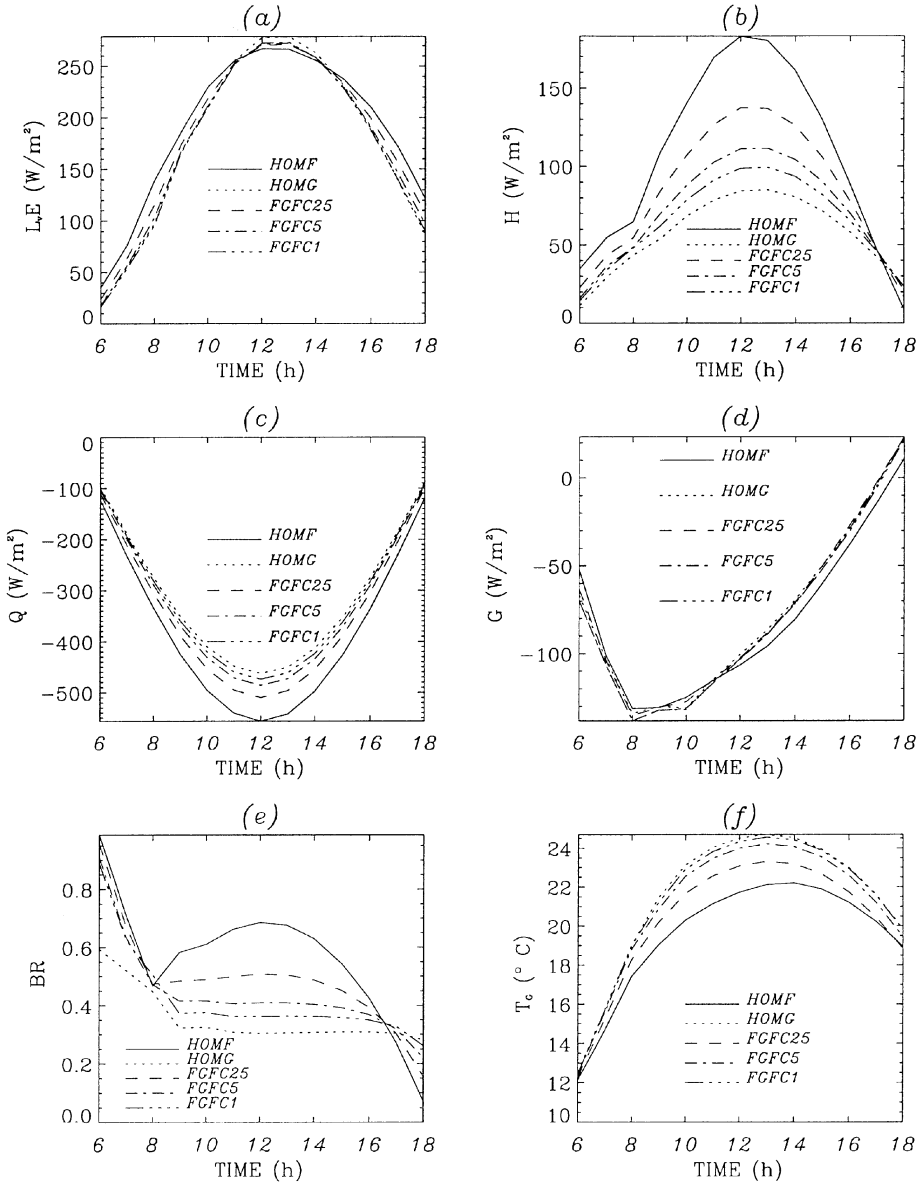

Fig. 3. Comparison of temporal development of the domain-averaged (a) latent heat-flux, L_vE, (b) sensible heat-flux, H, (c) net-radiation, Q, (d) soil heat-flux, G, (e) Bowen-ratio, BR, and (f) surface temperature, T_G

of all the synthetic landscapes examined here (Fig. 3c). Thus, incoming solar energy that can be partitioned between sensible and latent heat-fluxes differs for the various assumed landscapes. In the simulations with heterogeneous surface-cover, the domain-averaged net-radiation fluxes arrange themselves according to the fractional coverage of *grass* and *forest* (Fig. 3c). The differences between the domain-averaged net-radiation of HOMG and those of the simulations with heterogeneous surfaces increase with the decreasing heterogeneity and the increasing amount of *forest* (Fig. 3c).

Until noon, the sensible and latent heat-fluxes increase and reach their maximum between 12 LT and 13 LT (Fig. 3a, b), going along with the maximum of net-radiation (Fig. 3c). In the afternoon, net-radiation decreases and, therefore, the latent and sensible heat-fluxes decrease as well (Fig. 3a–c). Except between 12 LT and 13 LT, during the day, the highest domain-averaged latent heat-flux occurs for HOMF, while the lowest latent heat-flux is attained by HOMG (Fig. 3a). The latent heat-fluxes provided by the simulations assuming heterogeneous landscapes fall according to their amounts of *grass* and *forest*. These arrangements are caused mainly by differences in surface parameters and micrometeorological conditions (e.g., moisture-exchange coefficients, relative humidity, etc.) established

in the respective simulations. Between 12 LT and 13 LT, the domain-averaged latent heat-fluxes arrange themselves in the opposite way (Fig. 3a).

In the afternoon, the curves of the domain-averaged fluxes of latent and sensible heat do not coincide with those in the morning. This asymmetric behavior results from the altered thermal stratification of the near-surface ABL, the altered vertical mixing, and the soil which has been heating meanwhile (cf. Fig. 3f for surface temperature). The steepness of the curves of the domain-averaged latent and sensible heat-fluxes differs for the various landscapes. In the late afternoon, for instance, greater latent heat-fluxes are achieved in those simulations having a greater fractional coverage by *grass* than *forest* (Fig. 3b). The same is true for the fluxes of sensible heat in the early afternoon. However, in the late afternoon the opposite is true. This behavior means that a different degree of surface heterogeneity leads to an altered partitioning of net-radiation between sensible and latent heat where, moreover, the shift in the partitioning changes with the passing of time.

The results substantiate that ignoring the natural variability of surface conditions may lead to a greater margin of error in the predicted fluxes of sensible heat. In the case of FGFC25 and FGFC1, for instance, assuming the homogeneous surface characteristics of HOMG, the error amounts to 50 and 85 W/m^2, respectively. Note that the margin for error is minimal around 17 LT (Fig. 3b). At this time, the different micrometeorological conditions established cancel out. Later on, the different surface heterogeneity further alters micrometeorological conditions for which, again, differences arise.

4.2 The Bowen-Ratio

Since sunset forces a sudden decrease in net-radiation, the sensible and latent heat-fluxes run against zero. Thus, the Bowen-ratio achieves high or even meaningless values at that time. Therefore, only the daytime hours are considered in the further discussion. During daytime, the domain-averaged Bowen-ratios vary between values of 1 and 0.1 (Fig. 3e). In this case study, the prediction of the Bowen-ratio is governed mainly by the sensible heat-flux. Between 9 LT and 17 LT, the domain-averaged Bowen-ratios differ by about 0.05 and 0.2 in comparing HOMG and FGFC1 and for comparing HOMG and FGFC25, respectively. In this time range, the domain-averaged Bowen-ratio of HOMF exceeds that of HOMG by about 0.4, because of the higher sensible heat-fluxes over *forest* than *grass* (Fig. 3e). The domain-averaged Bowen-ratios provided by the simulations with heterogeneous surfaces reflect the fractional coverage by *grass* and *forest*. Moreover, they increase non-linearly for increasing fractional coverage by *forest* (Fig. 3e). Thus, neglecting surface heterogeneity may make for errors of several percentage points in the determination of a regional Bowen-ratio.

These findings are also supported by experimental data. Vukovich et al. (1997), for instance, investigated near-surface fluxes as a function of near-surface parameters and meteorological conditions with special focus on the variability of the near-surface fluxes within an area the size of a GCM grid-cell (global-circulation model). In so doing, the sensible and latent heat-fluxes were determined from meteorological and soil-specific properties provided by NOAA-AVHRR (advanced very-high-resolution radiometer) and by ground measurements as well as for different domain typical land-use-types. When assuming the dominant land-use-type as representative for the GCM-grid-cell area, the average margin for error was about 10% and 21% for the latent heat-flux and sensible heat-flux, respectively.

4.3 The Micrometeorological Conditions

Investigations on the influence of plant- (e.g., albedo, evaporative conductivity, etc.) and soil-specific parameters (e.g., albedo, heat capacity, thermal diffusivity of soil), meteorological conditions (e.g., insolation, near-surface humidity and air temperature), and soil conditions (e.g., soil wetness, soil temperature at various depth, thermal conductivity, etc.) have shown that the Bowen-ratio may react highly complexly and non-linearly to the changes in plant-physiological parameters and in meteorological and soil conditions (Friedrich, 1999).

As the diurnal cycle of ground temperature, among others, depends on land-use and soil-type, the domain-averaged ground temperature is also influenced by the dominating land-use and soil-

type (Fig. 3f). Generally, ground- and air temperatures directly influence the sensible heat-flux (Fig. 3f, b) and, hence, the Bowen-ratio (Fig. 3e).

The simulation results of FGFC25 or FGFC1 illustrate that assuming *grass* to be the representative surface type (represented by HOMG) leads to a misprediction of the domain-averaged air temperature (e.g., about 0.5 K and 1.5 K at noon, respectively).

The latent heat-flux depends on the difference between the specific humidity near the surface and that at reference height. Since air temperature and specific humidity are correlated exponentially, the Bowen-ratio varies non-linearly with changes in these quantities.

4.4 Normalized Energy-Budget

As mentioned previously, the variability in a region's surface governs the net-radiation of said region. Thus, the domain-averaged net-radiation differs for the various landscapes assumed (Fig. 3). Hence, in the distributions of latent and sensible heat-fluxes as well as soil heat-fluxes, some of the differences are due to the altered net-radiation (Fig. 3c). Consequently, the influence of surface heterogeneity on the latent and sensible heat-fluxes is eclipsed by the altered net-radiation (Fig. 3). To achieve better insight into the modified partitioning of net-radiation into the fluxes of latent and sensible heat, for each simulation these fluxes, the soil heat-fluxes as well as Bowen-ratios, are normalized by the simulated net-radiation according to

$$\Psi = \frac{100\chi}{Q}, \tag{2}$$

where χ stands for the fluxes of latent and sensible heat, the soil heat-fluxes, and the Bowen-ratios, respectively, and Ψ represents the normalized value χ in percent. This normalization allows for evaluating the sensitivity of the energy- and water-fluxes to the different heterogeneity (Fig. 4). Note that when comparing the results of two simulations, a higher percentage of a flux, Ψ, does not mean a higher absolute value in W/m^2 (cf. Fig. 3).

During the day, of all the energy-budget components it is the sensible heat-fluxes which react the most sensitively to changes in net-radiation (Fig. 4). The degree of heterogeneity governs the partitioning of net-radiation into the fluxes of sensible and latent heat (Fig. 4). In HOMF, for instance, net-radiation is divided into approximately 50% latent heat-flux, 35% sensi-

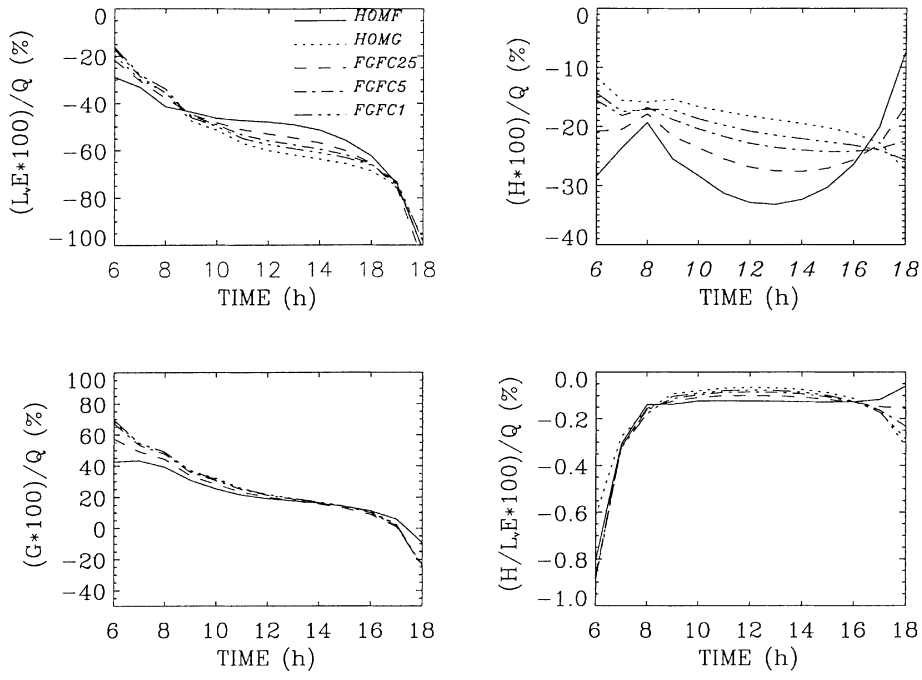

Fig. 4. Domain-averaged fluxes of latent heat, L_vE, sensible heat, H, and soil heat-flux, G, as well as the Bowen-ratio, H/L_vE, normalized by net-radiation, Q (in%)

ble heat-flux and 15% soil heat-flux at 12 LT. In HOMG, however, net-radiation is partitioned into approximately 65% latent heat-flux, 18% sensible heat-flux and 17% soil heat-flux at that time (Fig. 4). This means that the partitioning of net-radiation is shifted towards latent heat-flux when changed from *grass* to *forest*. In the case of heterogeneous landscapes, the partitioning of net-radiation into sensible and latent heat-fluxes shifts towards greater latent heat-fluxes for greater fractional coverage by *forest*.

Normalization clarifies that, between 8 LT to 17 LT, the fluxes of latent and sensible heat are the most strongly affected components of the energy-budget for a change in surface heterogeneity. Herein, moreover, a certain variability is observed during the day (Fig. 4). The highest sensitivity of the latent and sensible heat-fluxes to surface heterogeneity exists between 10 LT and 14 LT. The latent heat-flux varies approximately 13% in the net-radiation between a homogeneous *forest* domain and a homogeneous *grass* domain, while the variability of the sensible heat-flux is about 15% in the net-radiation at 12 LT. Only in the morning and in late afternoon, the soil heat-flux reacts sensitively to the different surface heterogeneity (Fig. 4).

Nevertheless, the normalized Bowen-ratio is only slightly affected by surface heterogeneity. This means that it is the net-radiation altered by heterogeneity and, hence, the altered albedo, which contribute mainly to the modified Bowen-ratio (cf. Figs. 3c, e, 4).

Applying the strategy of dominant surface type for all the heterogeneous landscapes assumed in this study results in *grass*, except for FGFC25. As mentioned above, the *grass*- and *forest*-patches have equal coverage in FGFC25. Thus, for this landscape, one has to decide whether to favor *grass* or *forest* to represent the area. Comparison of FGFC25 and HOMG (HOMF) at 12 LT, for example, shows that choosing *grass* as the representative surface type leads to a predictable margin for error of 12% (6%) in the net-radiation for the latent heat-flux, and nearly 9% (6%) in the net-radiation for the sensible heat-flux. If the strategy of dominant surface type is applied to the test domain in the cases of either FGFC5 or FGFC1, the predictable margin for error of latent and sensible heat-fluxes will slightly decrease.

5. The Horizontal Distribution of Bowen-Ratios

At noon, the Bowen-ratio of HOMG is about 0.3 over the whole domain, while it is about 0.7 for HOMF. Surface heterogeneity does indeed affect the Bowen-ratio, with the strongest impact occurring at 12 LT (Fig. 3e). Therefore, in this section the impact of heterogeneity on the Bowen-ratio distribution is examined at that time.

When determining a regional Bowen-ratio for a heterogeneous landscape, the natural surface variability would be suppressed by the strategy of dominant surface type. To illustrate the margin for error in the Bowen-ratio resulting from the strategy of dominant surface type, the Bowen-ratios obtained by FGFCx ($x = 1, 5, 25$) are subtracted from HOMG. Values close to zero may be expected if the surface type is the same (in this case *grass*) and is at the same location in both HOMG and FGFCx. Negative values (around 0.4) will occur if the patches are covered differently, because, according to both HOMG and HOMF, the *forest*-patches provide lower latent heat-fluxes at noon than do the *grass*-patches (Fig. 3a). Note that, as pointed out above, the micrometeorological conditions are not exactly the same due to advective effects. Figures 5 to 7 represent differences HOMG–FGFCx ($x = 25, 5, 1$). Herein, a positive value means a reduced Bowen-ratio in FGFCx as compared to HOMG.

The surface heterogeneity influences the near-surface atmosphere and the flow (see also Fig. 8) because of the altered surface characteristics (e.g., albedo, roughness length, emissivity, evaporative conductivity, etc.). Since the atmospheric moisture and temperature states try to be in an equilibrium with the respective underlying surface, the micrometeorological conditions (e.g., near-surface wind, near-surface temperature and humidity, etc.) are modified by fluxes whenever an air parcel passes a change in the underlying surface. Thus, after passing several changes of alternating patches of *grass* and *forest*, the micrometeorological conditions over a *grass*-patch located in the western part of the domain, for instance, differ slightly from those over *grass* in the eastern part of the domain because of the frequent modulation of the air mass. These

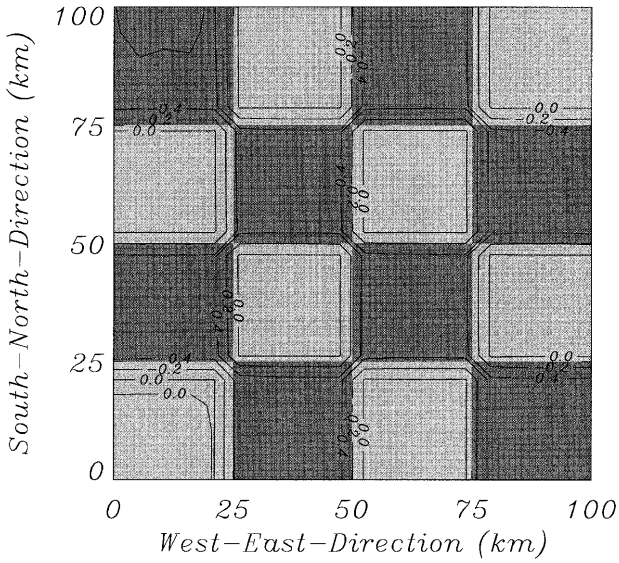

Fig. 5. Horizontal distribution of the Bowen-ratio at 12 LT for the difference between the results of HOMG and FGFC25. Dark grey patches indicate *forest* and light grey patches indicate *grass*

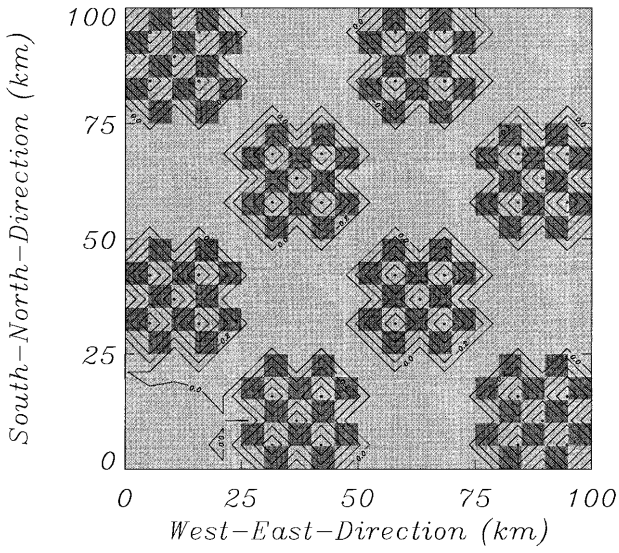

Fig. 6. Like Fig. 5, but for the difference between the results of HOMG and FGFC5

differences increase incrementally with time and distance from the first change in the underlying surface. The modified micrometeorological properties again modify the Bowen-ratio via altered sensible and latent heat-fluxes (e.g., Figs. 5–7).

Even in cases of identical land-use, different fluxes may occur within a large patch of *forest* or *grass*. This effect is due to the fact that the equilibrium between an air parcel which has

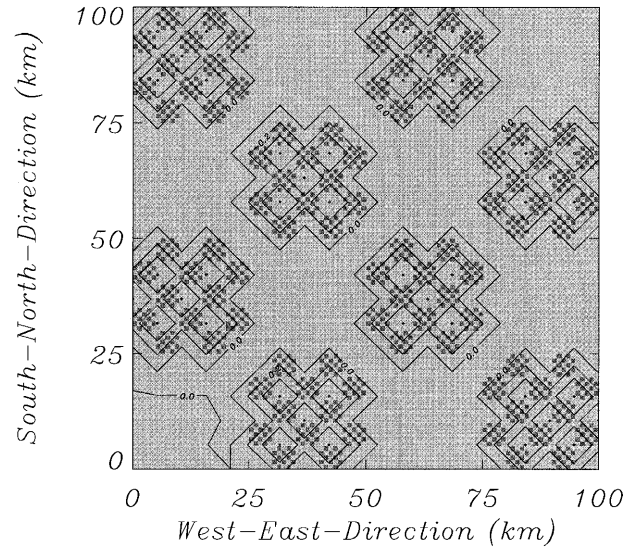

Fig. 7. Like Fig. 5, but for the difference between the results of HOMG and FGFC1

passed a discontinuity over the new underlying surface differs from that of an air parcel after a long passage over the same surface. Consequently, there is a shift in the pattern of fluxes of sensible and latent heat and, hence, in Bowen-ratio differences with respect to land-use patterns. With increasing heterogeneity, the near-surface atmosphere is influenced by the surface-specific conditions in the sense that, for short patches, less time exists to package the air mass by the characteristics of the underlying patch before the next patch begins.

Great differences in the Bowen-ratios of HOMG and FGFC1 arise (compare Figs. 5 and 7). Over regions with both heterogeneous surfaces and increasing heterogeneity and a decreasing amount of *forest* (Fig. 7), the Bowen-ratios provided by the simulations with heterogeneous surfaces approach those provided by the simulation with a homogeneous *grass* cover, HOMG. In the following subsections, the impact of heterogeneity on the distributions of Bowen-ratios will be elucidated in more detail.

5.1 Equal Fractional Coverage and Low Degree of Heterogeneity

As mentioned in Section 2, the fractional coverage of *forest* is equal to that of *grass* in FGFC25. The Bowen-ratios provided by FGFC25 increase during the transition from *grass* to *forest*, while

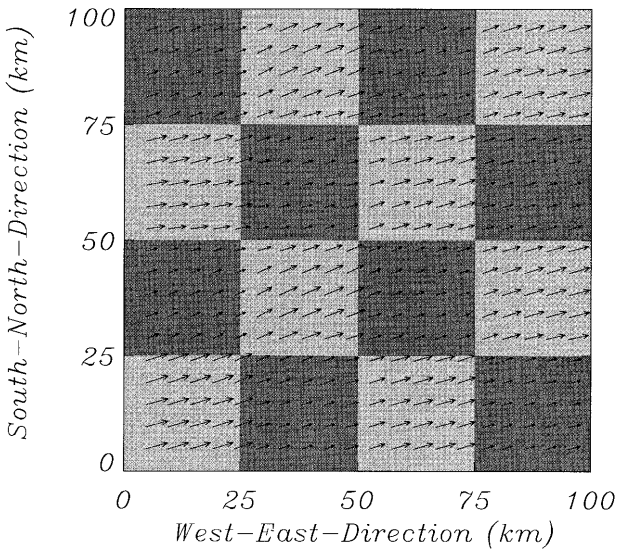

Fig. 8. Horizontal wind distribution of FGFC25 in the first level above ground at 12 LT. Dark grey patches indicate *forest* and light grey patches indicate *grass*. The mean windspeed amounts to about 5.4 m/s and 2.7 m/s above the *grass*- and *forest*-patches, respectively

they decrease during transition from *forest* to *grass* (Fig. 5). At the boundaries between the different patches, the modification of the Bowen-ratio shifts westwards during the time that the air flows over the domain. As explained above, this shift results from the effect of friction from the near-surface wind (Fig. 8) and forced continuously to adapt to the near-surface atmosphere to the always changing new micrometeorological and surface-specific conditions, i.e., the air mass is continuously modified when passing over the domain.

The aforementioned feedback between the micrometeorological properties and the fluxes, among others, contribute to the shift of the Bowen-ratio differences in a northeast to southwest direction. As an example of altered micrometeorological conditions, Fig. 8 illustrates the reduction in windspeed over a large *forest* area of $25\times25\,km^2$ and the increase in windspeed after passing the *forest*. The wind direction, however, is unaffected.

5.2 Medium Degree of Heterogeneity

In FGFC5, the Bowen-ratios vary between 0.3 (approximately the Bowen-ratio of HOMG), over to 0.7 (approximately the Bowen-ratio of HOMF), to a maximum value of 1.3. This strong increase in the Bowen-ratio occurs above the heterogeneous patches. The near-surface atmosphere over each $5\times5\,km^2$ *forest*-patch is found to be unable to build up turbulent fluxes that are independent of upwind conditions. Note that such behavior was proposed theoretically by Shuttleworth (1991). In that case, high Bowen-ratios do not occur exclusively above the *forest*-patches. The latent and sensible heat-fluxes react weakly to the heterogeneity (Fig. 6) at those positions where *forest* patches are surrounded mainly by *grass*. In the case of FGFC5, applying the strategy of dominant surface type leads to a margin for error in the Bowen-ratio of about 1 for the heterogeneous areas (Fig. 6). Note that a near equal margin for error will arise if the heterogeneous areas are assumed to be *forest*. One may conclude that if the surface of a landscape, region, or GCM grid-cell is very heterogeneous, no equilibrium between the atmosphere and the surface will be reached that is independent from upwind conditions.

5.3 High Degree of Heterogeneity

Considering the near-surface wind provided by FGFC1, the $25\times25\,km^2$-sized areas of patchy *forest*-islands in *grass* are too heterogeneous to provide a distinct response in the wind field. Therefore, the windspeed is hardly reduced over these heterogeneous areas (not shown). The mean windspeed amounts to about 5.3 m/s and 4.2 m/s above *grass*-areas and *grass*-areas with *forest*-islands, respectively. This insensitivity of the wind field to a high degree of heterogeneity may be explained partly by an artifact provided by the explicit subgrid-scheme that does not consider the heterogeneity of wind, air temperature and air-humidity on the subgrid (for a detailed discussion see Mölders et al., 1996). However, the fact that strongly heterogeneous surfaces, i.e., smallness of patch-size, provide no distinct response to the atmosphere is also substantiated by sensitivity studies performed with different surface patterning types other than those discussed above as well as by studies with a higher degree of heterogeneity and higher resolution than what is presented here.

Compared with other simulation results, the absolute values of the Bowen-ratio distribution of

FGFC1 do not arrange themselves according to any degree of heterogeneity. FGFC1 is the only case in which the maximal value of the Bowen-ratio decreases with the increasing heterogeneity over the heterogeneously covered $25\times25\,\mathrm{km}^2$ patches. Over the $5\times5\,\mathrm{km}^2$ patches covered heterogeneously, the area-averaged Bowen-ratio value is about 0.9, and the distribution pattern of the Bowen-ratio values is nearly the same as in FGFC25.

With reference to the pattern of the Bowen-ratio of FGFC1 alone, however, there are similarities to the pattern obtained by the simulation with the wider horizontal patch sizes of $5\times5\,\mathrm{km}^2$ (FGFC5), that is to say, although the values of FGFC1 and FGFC5 differ, the spatial pattern provided by these simulations remains the same.

5.4 Similarity

For comparing data fields containing different parameters or for comparing data fields with the same parameters but recorded at different times, Ogunjemiyo et al. (1997) modified a given procedure by Jackson et al. (1989). In our case study, this modified procedure is adapted in order to compare the results obtained by the simulations with a different surface heterogeneity (for details, see Friedrich, 1999). In doing so, the variables (e.g., Bowen-ratio, ground temperature, etc.), A_{ij}, at the grid-point i,j on the distribution field, are transformed into a set of values Z_{ij}, by subtracting the domain-averaged value and normalizing the difference by the standard deviation of the differences S (see Ogunjemiyo et al., 1997; Friedrich, 1999)

$$Z_{ij} = \frac{A_{ij} - \overline{A}}{S}. \tag{3}$$

The similarity between two transformed distributions is now established on the basis of similarity in the sign of $Z_{i,j}$ pairs (Ogunjemiyo et al., 1997; Friedrich, 1999) as

$$C_s = \frac{m+n}{m+n+p}. \tag{4}$$

Here, C_s is the similarity coefficient, and m, n, and p are the numbers of Z_{ij} pairs with negative, positive, and mixed signs. The similarity coefficient varies between zero (no similarity) and 1 (absolute agreement). Application of the similarity coefficients points out those landscapes which yield similar results with respect to the regional Bowen-ratio. Furthermore, the time variance of these quantities caused by different landscapes can be detected (Table 2).

Table 2. *Comparison of the Similarity Coefficients C_s for all Simulations at 12 LT, 15 LT and 18 LT. The Upper Triangle of the Table Represents the Similarity Coefficients for the Bowen-ratio BR, the Lower Triangle Locates the Similarity Coefficients for the Surface Temperature T_G*

BR 1200 LT \ 1500 LT T_G 1800 LT	HOMF	HOMG	FGFC25	FGFC5	FGFC1
HOMF		0.31	0.68	0.64	0.66
		0.49	0.64	0.71	0.71
		0.66	0.49	0.45	0.48
HOMG	0.79		0.38	0.40	0.39
	0.54		0.32	0.28	0.26
	0.38		0.57	0.58	0.54
FGFC25	0.49	0.49		0.87	0.98
	0.49	0.50		0.86	0.89
	0.48	0.48		0.47	0.54
FGFC5	0.68	0.60	0.74		0.89
	0.51	0.70	0.74		0.96
	0.36	0.67	0.72		0.67
FGFC1	0.68	0.60	0.74	1	
	0.50	0.72	0.73	0.99	
	0.35	0.56	0.57	0.85	

As mentioned above, in the case of a coarse resolution of about $100 \times 100\,\mathrm{km}^2$ and the strategy of dominant surface type, *grass*-covered loam would be used to simulate the exchange of matter, heat and moisture at the interface *earth-atmosphere* in FGFC5 and FGFC1. According to the calculated similarity coefficients (Table 2), especially, this strategy of dominant surface type leads to the worst representation of the regional Bowen-ratio for FGFC5 and FGFC1, respectively. Here, even determining the fluxes by assuming a dominance of *forest* (HOMF) would provide a better estimate of the regional Bowen-ratios for FGFC5 and FGFC1 than assuming *grass* to be the representative surface type (Table 2). This is due especially to the fact that *forest* influences the whole domain persistently because of its considerable roughness length. Thus, vertical mixing and stratification are strongly influenced by the presence of even small patches of *forest*.

Note that an adequate behavior is found for other quantities, for instance, ground temperature (Table 2). The differences in the domain-averaged ground temperatures between HOMG, HOMF, FGFC25 and FGFC5 are quite large, whereas, according to the similarity coefficients, FGFC5 and FGFC1 hardly differ in both Bowen-ratio and ground temperature. The latter may suggest that, for the determination of the mean Bowen-ratio representative for an area of $100 \times 100\,\mathrm{km}^2$, a lower limit might be sufficient for the required resolution of the data. The highest agreement ($C_s > 0.8$) between simulations with different degrees of heterogeneity (between FGFC25 and FGFC5, FGFC25 and FGFC1, FGFC5 and FGFC1) is found during 12 LT and 15 LT.

6. Conclusion

In the theoretical case study presented here, the influence of surface heterogeneity on the Bowen-ratio is examined by various methods (temporal and spatial distribution, normalization in the net-radiation, similarity coefficients). The results substantiate that:

- The horizontal distribution of Bowen-ratios depends on surface heterogeneity. This dependence is non-linear in space and time.
- The hourly domain-averaged (= regional) Bowen-ratio values depend mainly on the amount of *grass* or *forest* existing within the area under examination.
- In the case of heterogeneous regions, the domain-averaged (= regional) Bowen-ratio cannot necessarily be attained by area-weighting the number of patches of different land-uses and soil-types because the near-surface meteorological conditions (wind, air temperature, humidity) are modified by the heterogeneity in the upwind regions.
- The heterogeneity changes the domain-averaged net-radiation. The percentage partitioning of the domain-averaged net-radiation into sensible and latent heat, however, differs with each different degree of heterogeneity.
- According to the similarity coefficients, the dominant surface type may not be the representative one. With limitation of FGFC25 (equal fractional coverage by *forest* and *grass*), HOMG would be the landscape according to the strategy of the dominant surface type. However, no agreement ($C_s < 0.4$) in the horizontal Bowen-ratio distribution is reached between HOMG and FGFCx ($x = 1, 5, 25$).
- The similarity coefficients show that the Bowen-ratios determined for the various heterogeneous landscapes are more similar to each other than to those of the landscapes covered by only one surface type. The highest agreement ($C_s > 0.8$) between simulations with a different degree of heterogeneity (between FGFC25 and FGFC5, FGFC25 and FGFC1, FGFC5 and FGFC1) is found during 12 LT and 15 LT.

Based on these findings, it may be concluded that neglecting surface heterogeneity (e.g., by applying the strategy of dominant surface types) may lead to a misprediction of the mean Bowen-ratio representative for an area.

The Bowen-ratio normalized by net-radiation is hardly affected by heterogeneity between 9 LT and 17 LT. This finding reveals that the change in net-radiation due to the altered heterogeneity is what mainly contributes to the altered Bowen-ratio. The surface characteristics that influence net-radiation, however, are albedo.

Based on the finding that, although *forest* is not the dominant surface type in FGFC5 and

FGFC1, respectively, the results of these simulations are more similar to those of HOMF than to those of HOMG, and one may conclude that roughness length may also play a role by way of the altered mixing and stratification. Thus, height of canopy also seems to be important for determining the Bowen-ratio.

Moreover, the results suggest that the data-resolution has to be very carefully chosen with respect to the heterogeneity of the landscape in order to determine an adequate regional Bowen-ratio. In modeling studies, for instance, this means that a fine grid-resolution will be favored if enough computer time and storage capacity are available.

As pointed out above, the results of this study also suggest that Bowen-ratio distributions do not depend only on the underlying surface and local characteristics alone. Feedback processes occur between the components of the near-surface energy-budget, the atmosphere, and the current flow. Therefore, in experimental as well as numerical studies, this dependence on the surrounding properties, as well as on the surface characteristics, has to be considered, and maps of Bowen-ratios should be determined either by use of (temporally and spatially) highly resolved observational data or by means of 3-D-simulations. Note that, if the observation network has a high resolution, measured data will include the upwind effects of heterogeneity.

Acknowledgments

We would like to express our thanks to Peter Schuepp, Thomas Foken, and the reviewers for fruitful discussions and helpful comments. We also thank Nerissa Röhrs for help with the language. Thanks also to the DFG (contracts Mo770/1-1 and Mo770/1-2) and the BMBF (contract LT2.D2) for financial support of this study.

References

Claussen, M., 1988: On the surface energy budget of coastal zones with tidal flats. *Contrib. Atmos. Phys.,* **61**, 39–49.

Deardorff, J. W., 1978: Efficient prediction of ground surface temperature and moisture, with inclusion of a layer of vegetation. *J. Geophys. Res.,* **84C**, 1889–1903.

Devantier, R., Raabe, A., 1996: Application of a quasispectral cloud parameterization scheme to a mesoscale snowfall event over the Baltic Sea. *Contrib. Atmos. Phys.,* **69**, 375–384.

Entekhabi, D., Brubaker, K. L., 1995: An analytical approach to modeling land-atmosphere interaction. 2. Stochastic formulation. *Water Resource Res.,* **31**, 633–643.

Eppel, D. P., Kapitza, H., Claussen, M., Jacob, D., Koch, W., Levkov, L., Mengelkamp, H.-T., Werrmann, N., 1995: The non-hydrostatic mesoscale model GESIMA. Part II: Parameterizations and applications. *Contrib. Atmos. Phys.,* **68**, 15–41.

Friedrich, K., 1999: Numerische Untersuchungen zur Sensitivität des Bowen-Verhältnisses. *Master Thesis, Inst. Meteorologie, Univ. Leipzig (available from the author).*

Fritsch, H., 1999: Parametrisierung von Bodenfeuchte und Bodentemperatur für ein mesoskaliges Modell. *Master Thesis, Inst. Meteorologie, Univ. Leipzig (available from the author).*

Foken, Th., Richter, S., Müller, H., 1997: The accuracy of the Bowen-ratio method. *Wetter und Leben,* **49**, 57–77.

Giorgi, F., Avissar, R., 1997: Representation of heterogeneity effects in earth system modeling: Experience from land surface modeling. *Rev. Geophys.,* **35**, 413–438.

Hinneburg, D., Tetzlaff, G., 1996: Calculated wind climatology of the South-Saxonian/North-Czech mountain topography including an improved resolution of mountains. *Ann. Geophysicae,* **14**, 767–772.

Jackson, D. A., Somers, K. M., Harvey, H. H., 1989: Similarity coefficients: Measures of co-occurrence and association or simply measures of occurrence? *Am. Natur.,* **133**, 436–453.

Jarvis, P. G., 1976: The interpretation of the variations in leaf water potential and stomatal conductance found in canopies in the field. *Phil. Trans. R. Soc. Lond.,* B., **273**, 593–610.

Kapitza, H., Eppel, D. P., 1992: The non-hydrostatic mesoscale model GESIMA. Part I: Dynamical equations and tests. *Contrib. Phys. Atmos.,* **65**, 129–146.

Kramm, G., Dlugi, R., Dollard, D. J., Foken, T., Mölders, N., Müller, H., Seiler, W., Sievering, H., 1995: On the dry deposition of ozone and reactive nitrogen compounds. *Atmos. Environ.,* **29**, 3209–3231.

Mölders, N., Raabe, A., 1996: Numerical investigations on the influence of subgrid-scale surface heterogeneity on evapotranspiration and cloud processes. *J. Appl. Meteor.,* **35**, 782–795.

Mölders, N., Raabe, A., Tetzlaff, G., 1996: A comparison of two strategies on land surface heterogeneity used in a mesoscale β meteorological model. *Tellus,* **48A**, 733–749.

Mölders, N., 1998: Landscape changes over a region in East Germany and their impact upon the processes of its atmospheric water-cycle. *Meteorol. Atmos. Phys.,* **68**, 79–98.

Mölders, N., Kramm, G., 1999: On the influence of the parameterization of soil and vegetation processes upon the simulated evapotranspiration. In: Fohrer, N., Döll, P. (eds.) *Modellierung des Wasser- und Stofftransports in großen Einzugsgebieten*. Kassel: University Press, pp. 163–172.

Müller, H., Kramm, G., Meixner, F., Fowler, D., Dollard, G. J., Possanzini, M., 1993: Determination of HNO_3 dry deposition by modified Bowen-ratio and aerodynamic profile techniques. *Tellus,* **45B**, 346–367.

Ogunjemiyo, S., Schuepp, P. H., MacPherson, J. I., Dejardins, R. L., 1997: Analysis of flux maps versus surface characteristics from Twin Otter grid flights in BOREAS 1994. *J. Geophys. Res.,* **102**, 29135–29145.

Panin, G. N., Raabe, A., Tetzlaff, G., 1998: Inhomogeneity of the land surface and problems in parameterization of surface fluxes in natural conditions. *Theor. Appl. Climatol.,* **60**, 163–178.

Seth, A., Giorgi, F., Dickinson, R. E., 1994: Simulating fluxes from heterogeneous land-surfaces: explicit subgrid method employing the biosphere-atmosphere transfer scheme (BATS). *J. Geophys. Res.,* **99D**, 18651–18667.

Shuttleworth, W. J., 1991: Insight from large-scale observational studies on land/atmosphere interactions. *Surveys in Geophysics,* **12**, 3–30.

Vukovich, F. M., Wayland, R., Toll, D., 1997: The surface heat-flux as a function of ground cover for climate models. *Mon. Wea. Rev.,* **125**, 572–586.

Authors' addresses: Katja Friedrich*, Nicole Mölders, Gerd Tetzlaff, LIM–Institut für Meteorologie, Universität Leipzig, Stephanstrasse 3, D-04103 Leipzig, Germany; * Present affiliation: DLR, Institut für Physik der Atmosphäre, Oberpfaffenhofen, Postfach 1116, D-82230 Wessling, Germany.